DR JOSÉ M. TORRES-RUIZ (Orcid ID : 0000-0003-1367-7056)

DR PAULO EDUARDO MENEZES-SILVA (Orcid ID : 0000-0002-8122-3489)

Article type : Regular Manuscript

Where do leaf water leaks come from? Trade-offs underlying the variability in minimum conductance across tropical savanna species with contrasting growth strategies

Renan Machado[1], Lucas Loram-Lourenço[1], Fernanda Santos Farnese[1], Rauander Douglas Ferreira Barros Alves[1], Letícia Ferreira de Sousa[1], Fabiano Guimarães Silva[1], Sebastião Carvalho Vasconcelos Filho[1], José M. Torres-Ruiz[2], Hervé Cochard[2], Paulo Eduardo Menezes-Silva[1]*

[1]Laboratory of Plant Physiology, Department of Biology, Federal Institute of Education, Science and Technology Goiano, Campus Rio Verde, 75901-970 Rio Verde, Brazil

[2]Université Clermont-Auvergne, INRAE, PIAF, 63000 Clermont-Ferrand, France

ORCID IDs: 0000-0001-5408-5853 (LL-L); 0000-0002-5373-9007 (FSF); 0000-0001-8931-1806 (RDFBA); 0000-0001-5357-8752 (LFS); 0000-0003-4908-2265 (FGS); 0000-0002-2061-7062 (SCVF); 0000-0003-1367-7056 (JMT-R); 0000-0002-2727-7072 (HC); 0000-0002-8122-3489 (PEM-S)

***Author for correspondence**

Paulo Eduardo Menezes-Silva

Tel.: +55 64 36205600

E-mail: paulo.menezes@ifgoiano.edu.br

Received: 10 May 2020
Accepted: 4 September 2020

Summary

- Plants continue to lose water from their leaves even after complete stomatal closure. Although this minimum conductance ($g_{\text{leaf-res}}$) has substantial impacts on strategies of water use and conservation, little is known about the potential drivers underlying the variability of this trait across species.
- We thus untangled the relative contribution of water leaks from the cuticle and stomata in order to investigate how the variability in leaf morphological and anatomical traits is related to the variation in $g_{\text{leaf-res}}$ and carbon assimilation capacity across 30 diverse species from the Brazilian Cerrado.
- In addition to cuticle permeance, water leaks from stomata had a significant impact on $g_{\text{leaf-res}}$. The differential patterns of stomata distribution in the epidermis was a key factor driving this variation, suggesting the existence of a trade-off between carbon assimilation and water loss through $g_{\text{leaf-res}}$. For instance, higher $g_{\text{leaf-res}}$, observed in fast-growing species, was associated with the investment in small and numerous stomata, which allowed higher carbon assimilation rates but also increased water leaks, with negative impacts on leaf survival under drought. Variation in cuticle structural properties was not linked to $g_{\text{leaf-res}}$.
- Our results therefore suggest the existence of a trade-off between carbon assimilation efficiency and dehydration tolerance at foliar level.

Key words: Cerrado, carbon assimilation, cuticle permeance, hydraulic failure, minimum transpiration, leaf mortality, stomatal density.

Introduction

Relative to all the resources needed to sustain plant growth and development, water is probably the most abundant and, at the same time, the most limiting. In fact, water availability is the main factor determining the performance, distribution, and survival of plant species worldwide (Choat *et al.*, 2012; Anderegg, 2015; Klein *et al.*, 2015; Trueba *et al.*, 2017). Under conditions of water restriction, plants typically reduce the aperture of their stomata (reduction in stomata conductance – g_s), a strategy that significantly lowers water loss through transpiration but, at the same time, limits the CO_2 diffusion for photosynthesis (Galmés *et al.*, 2013; Xiong *et al.*, 2016). Thus, plants must constantly cope with the trade-off of maximizing the CO_2 diffusion while minimizing the water lost through transpiration (Mcadam & Brodribb, 2012). However, even after complete stomatal closure, plants keep losing water to the atmosphere. This residual transpiration rate, also described by its minimum conductance (hereafter referred as $g_{\text{leaf-res}}$), represents an inevitable water leak, which has a great impact on the strategies of water use and conservation across species (Kerstiens, 1996a; Martin-StPaul *et al.*, 2017; Duursma *et al.*, 2019). In fact, recent studies have suggested $g_{\text{leaf-res}}$ as a key trait determining the survival under drought conditions, such that species with lower $g_{\text{leaf-res}}$ tend to sustain a better water status, postponing hydraulic failure and drought-induced mortality, when compared to plants with higher $g_{\text{leaf-res}}$ rates (Gleason *et al.*, 2014; Cochard, 2019; Duursma *et al.*, 2019). However, despite the impact of $g_{\text{leaf-res}}$ on the strategies of water use and conservation, little is known about how differences in leaf functional properties are related to the high variability of this trait across species (Schuster *et al.*, 2017).

Different lines of evidence suggest that water loss from minimum transpiration arises from leaks at two main sites: cuticle and stomata (Kerstiens, 1996b; Richardson *et al.*, 2007; Bueno *et al.*, 2019). The plant cuticle covers the outer cell walls of the leaf epidermis, serving to reduce water loss, as well as protect against pathogens and UV damage (Kerstiens, 1996a; Schuster *et al.*, 2017). Chemically, the cuticle can be described as a polymer membrane composed of a cutin matrix and cuticular waxes (Schuster *et al.*, 2017). The water loss through the cuticle only (i.e. when leaks from stomata are not considered) is termed cuticular transpiration (and determined by its conductance - g_{cuticle}) and involves the dissolution of water molecules inside the leaves into the medium of the cuticle, their diffusion through the solid matrix and, finally, the desorption from the cuticular waxes at the outer portion of this membrane (Richardson *et al.*, 2007; Duursma *et al.*, 2019). Given the diversity of ecological functions assumed by the cuticle, it is expected that differences in the relative investment in this structure, as a consequence of contrasting growth strategies, for example, would largely influence the variability in $g_{\text{leaf-res}}$ across species, a hypothesis not always experimentally supported (Kerstiens, 1996a; Richardson *et al.*, 2007).

The contribution of stomatal leakiness to the $g_{\text{leaf-res}}$ rates is far less studied than those from the cuticle (Duursma *et al.*, 2019). In fact, although it was already shown that in hypostomatous leaves the water leaks from the abaxial side (stomatous surface) tend to be much higher than those on the adaxial side (solid cuticle) (Brodribb *et al.*, 2014), few studies have focused on the factors that drive such differences in water permeability on those leaves (Duursma *et al.*, 2019). Some evidence suggests that this higher water permeability in the stomatous leaf surface arises from the combination of incomplete stomatal closure, and the permeability of the cuticle that covers the guard cells, which leads to a higher stomatal residual transpiration (g_{stomata}) (Schuster *et al.*, 2017). Thus, if stomata have such an impact on determining $g_{\text{leaf-res}}$ rates, it could be expected that variations in its size (*SS*) and density (*SD*) would largely affect this trait. In fact, strong positive correlations between *SD* and $g_{\text{leaf-res}}$ were already reported for 10 Sorghum varieties (Muchow & Sinclair, 1989), a result that supports the "leaky stomata" hypothesis (Šantrůček *et al.*, 2004). Besides that, as changes in *SS* and *SD* are major determinants of the maximum leaf diffusive conductance to CO_2 and water vapor (g_{wmax} and g_{cmax}, respectively) (Franks *et al.*, 2009), we also could expect that contrasting strategies of carbon assimilation and water use should be reflected on $g_{\text{leaf-res}}$ rates. Although never experimentally tested, this observation suggests the existence of a trade-off between carbon assimilation and minimum conductance.

As both cuticle and stomata are extremely responsive to variation in environmental conditions, especially to water availability (Duursma *et al.*, 2019), species inhabiting regions with periodic drought episodes should present high variability in g_{leaf} rates, which would reflect their contrasting strategies of water use and conservation. This might be the case of the plants which inhabit the Cerrado, the second-largest Brazilian biome and one of the world's largest biodiversity hotspots (Strassburg *et al.*, 2017). The climate of Cerrado is characterized by a long period of water restriction, approximately five months. These climate conditions possibly acted as an important selective pressure that shaped several plant lineages that successfully invaded savannah environments, such that they differ in their morphological and physiological traits, especially with respect to the investment in wood, bark, and leaves (Rossatto & Franco, 2017; Loram-lourenço *et al.*, 2020). Interestingly, most of the plants of this domain are drought deciduous, and thus shed their leaves during periods of water shortage (Franco *et al.*, 2005). As differences in leaf habit usually reflect contrasting strategies of carbon assimilation and water use among co-occurring species (Poorter *et al.*, 2009; Villar *et al.*, 2016; John *et al.*, 2017), we can expect that differences in deciduousness in the Cerrado vegetation possibly involve a differential investment in cuticle and stomata, with a direct impact on $g_{\text{leaf-res}}$ rates across species. However, to the best of our knowledge, no studies to date have explored how the variation in $g_{\text{leaf-res}}$ rates can be explained by differences in cuticular and stomatal properties of species with contrasting growth strategies.

The main objective of the present study was to characterize the $g_{\text{leaf-res}}$ variability among species showing different life-history strategies and to better understand which are the main anatomical and morphological characteristics that drive this presumably high variability. To achieve this objective, 30 native species, widely distributed in the Cerrado, were analyzed to answer the following questions: *i*) How does variation in cuticular and stomatal traits affect the $g_{\text{leaf-res}}$ rates across species? As the cuticle represents a key barrier to water loss, and stomata the main leaks, we hypothesized that a combination of a thinner leaf cuticle in association with higher *SD* will be associated with higher $g_{\text{leaf-res}}$ rates. ii) What are the benefits and costs associated with high $g_{\text{leaf-res}}$ rates? Considering that both *A* and $g_{\text{leaf-res}}$ rates are affected by stomata dimensions and frequency, we predicted that the variability in $g_{\text{leaf-res}}$ rates would arise from an inevitable trade-off between carbon assimilation and water loss. In this regard, to achieve higher *A* rates, fast-growing species will cover their leaf epidermis with a high number of small stomata, which ultimately will lead to high $g_{\text{leaf-res}}$ rates, due to stomata leakiness. iii) If $g_{\text{leaf-res}}$ is related to carbon economics and water use and conservation, will this trait be reflected in different life-history strategies? We hypothesized that, as a result of their fast-growing strategy, deciduous species will have a set of morphological and anatomical characteristics, including cuticle and stomata, which would enable a higher carbon assimilation rate but, at the same time, would lead to higher water loss when compared to evergreen species.

Material and Methods

Study site and species selection

To understand the ecological consequences of the variability in $g_{\text{leaf-res}}$ rates, 30 representative tree species of the Cerrado biome were sampled. All sampling and analyses were performed on a natural population of a Cerrado fragment belonging to the ecological reserve of the University of Rio Verde, Rio Verde, Goiás (GO), Brazil (17°47'09.2" S 50°57'50.63" W). The mean annual precipitation in the reserve is 1700 mm, with the dry season extending from May to September, and the mean annual temperature is 23 ºC. The species selected were the most abundant in the region, and four adult plants of each species were analyzed. The selected species cover a diversity of families (Table 1) and encompass substantial structural and functional variability, which ensured a broad representation of the Cerrado tree flora. All the morphological and physiological analyses were conducted during the rainy season, between February and April, using the youngest, fully expanded leaves, which correspond to the third or fourth leaf pair from the apex of lateral branches.

Leaf mass area

The leaf mass area (LMA) was calculated as the ratio between leaf area and dry mass. All the sampled leaves for LMA measurements were fully expanded and did not show signs of mechanical or pathogen damage (Markesteijn *et al.*, 2011).

Stomatal characterization

The epidermal impression technique was used to determine the stomatal properties (Franks *et al.*, 2009). Fully expanded leaves were sampled in the field, between 08:00 and 10:00 am, re-cut under pure water, and brought to the laboratory. In the detached leaves, a small amount of instant glue was placed on a histological slide, and the vegetable material (adaxial and abaxial leaf side) was pressed against the slide for a few minutes. Then, the slides were observed at 20x magnification with the aid of a light microscope (model AX70TRF, Olympus, Tokyo, Japan). It is important to note that, after careful inspection of the patterns of stomatal distribution on both leaf sides, it was found that all sampled species were hypostomatous, and thus all stomatal measurements described in the lines bellow were performed only on the abaxial leaf side.

In each slide, a minimum of 5 images per field was taken at 100x and 400x magnification to determine the stomatal density (*SD*), guard cell length (*L*), guard cell pair width (*W*), and stomatal pore length (*p*), using the ImageJ software (Franks *et al.*, 2009; Galmés *et al.*, 2013). The stomatal size (*SS*) was determined using the *L* and *W* measurements. The theoretical maximum stomatal conductance (g_{wmax}) was calculated based on these data as proposed by Franks et al. (2009):

$$\mathrm{g}_{wmax} = \frac{SD.d_w.a_{max}}{v\left(l + \frac{\pi}{2}\sqrt{\frac{a_{max}}{\pi}}\right)}$$

where d_{w} represents the diffusion coefficient of water vapor in air, a_{max} is the maximum pore area of fully open stomata, v is the molar volume of air, and l represents the pore depth of a fully opened stomata. For normalization of the values, the constants d_{w} and v represent the values at 25°C (24.9 x 10^{-6} m^2 s^{-1} and 24.4 x 10^{-3} m^3 mol^{-1}, respectively). a_{max} was calculated as π $(\rho/2)^2$, according to Franks et al. (2009). l for a fully opened stomata was taken as $L/4$ assuming guard cells to inflate to circular cross-section (Franks *et al.*, 2009). In addition, the average fraction of the leaf epidermis that is allocated to stomata (f_{gc}) was determined by the average area of the guard cell pair (a_{gc}) and average stomatal density (de Boer *et al.*, 2016).

$$f_{gc} = a_{gc}.SD$$

where a_{gc} was calculated as:

$$a_{gc} = \frac{\pi}{2}.W.L$$

Cuticle thickness

Leaf cuticle thickness was determined by hand sectioning fresh leaves. One section of the middle lamina was stained with Sudan III solution (Bacelar *et al.*, 2004; Gotsch *et al.*, 2010). After the staining, the segments were observed and photographed at 200x and 400x magnification (Supporting Information Fig. S1) with the above-mentioned microscope. The thickness of the adaxial ($\mathrm{CT}_{\mathrm{adaxial}}$) and abaxial ($\mathrm{CT}_{\mathrm{abaxial}}$) cuticle were made at multiple points along the leaf cross-section and reported as averages per leaf. The total cuticle thickness (CT_{total}) was expressed as the average mean values of $CT_{adaxial}$ and $CT_{abaxial}$.

Water leaks: minimum transpiration rates

Leaf minimum water conductance ($g_{leaf\text{-}res}$) was determined gravimetrically from the consecutive weight loss of desiccating leaves (Slavik 1974; Sack et al., 2003). Before analysis, high-melting-point (68 °C) paraffin wax was used to seal the wounds of cut petioles of water-saturated leaves. Leaves were dried on a bench laboratory under dark conditions, to induce stomatal closure, and weighted at regular intervals (45-60 min). Leaf minimum transpiration was measured as the slope of water loss versus time, normalized by the total leaf surface area (sum of the adaxial and abaxial projected areas). For the slope estimation, only the linear part of the regression was used ($R^2 > 0.99$), which usually included the points after hours of dehydration (e.g. 3 hours), suggesting maximal stomatal closure (Billon *et al.*, 2020). The value of $g_{leaf\text{-}res}$ was calculated as cuticular transpiration/mole fraction gradient in water vapor from the leaf to air (Slavik, 1974; Sack *et al.*, 2003; Schuster *et al.*, 2017), assuming the leaf internal air to be fully saturated (Percy *et al.*, 2000; Sack *et al.*, 2003) (see Supporting Information Methods S1 for further details). Ambient temperature and relative humidity (RH), measured at 30 min intervals with a digital thermal hygrometer, varied minimally during the measurements, and the differences in RH for measurements of different species were not in the range that would significantly affect $g_{leaf\text{-}res}$ (Schreiber, 2001; Sack *et al.*, 2003) (Supporting Information Table S1).

To disentangle the relative contribution of water leaks arising from cuticle and stomata to the overall variation in minimum conductance across species, we decomposed $g_{leaf\text{-}res}$ to its main components (Fig. 1). For this, after the initial $g_{leaf\text{-}res}$ measurement, multiple layers of petroleum jelly were applied to the abaxial leaf surface, and water loss was measured again, as described above until a new stabilization point was reached (Brodribb *et al.*, 2014). As all the selected species were hypostomatous, the sealing of the abaxial (stomatous) surface allowed to achieve the minimum transpiration through the cuticle only (cuticular transpiration of the adaxial leaf side - $g_{cuti\text{-}adaxial}$). Finally, multiple coats of petroleum jelly were applied to the adaxial surface, and the water leaks through the jelly were measured (g_{leaks}) (Brodribb *et al.*, 2014). The minimum transpiration of the abaxial leaf side ($g_{abaxial}$) was then calculated based on the known values of $g_{leaf\text{-}res}$, $g_{cuti\text{-}adaxial,}$ and g_{leaks}, assuming that each leaf surface was composed of a series of unknown resistors in parallel to water diffusion (adaxial and abaxial surface resistance and leakiness of the jelly), as described by Brodribb et al. (2014). To derive the cuticular transpiration from the abaxial leaf side ($g_{\text{cuti-abaxial}}$), we first estimated the cuticle area from the abaxial leaf surface by removing the area occupied by stomata (based on the anatomical determinations described above) from the projected leaf area. The $g_{\text{cuti-abaxial}}$ was then calculated as $g_{\text{cuti-adaxial}}$ normalized by cuticle area from the abaxial leaf side, assuming that the cuticle from both leaf sides has the same chemical composition and thus similar water permeance (see Supporting Information Methods S1 for further details). After the estimation of $g_{\text{cuti-abaxial}}$, the minimum conductance from stomata (g_{stomata}), which integrates the water leaks from stomata pore due to incomplete closure ($g_{\text{stomata-pore}}$), and the diffusion of water through guard cells ($g_{\text{peristomatal}}$), was derived as:

$$g_{\text{stomata}} = g_{\text{abaxial}} - g_{\text{cuti-abaxial}}$$

Gas exchange

The net carbon assimilation rate *(A)*, stomatal conductance (g_s), and the transpiration rate (E) were determined in an open system under saturated light conditions (1500 µmol photons m^{-2} s^{-1}), temperature of 25 °C and a CO_2 partial pressure of 40 Pa using an infrared gas analyzer (LI-6800, LI-COR, Nebraska, USA) equipped with a blue/red light source. Gas exchange measurements were conducted in two consecutive days (e.g. two leaves of each species per day, four leaves in total), between 08:00 and 11:00 am in sun-exposed, fully expanded leaves. Climate conditions remained stable through the measurement days, with no significant variation in mean air temperature or relative humidity.

Statistical analysis and modeling approach

Before analysis, species traits were $\log_{10}$-transformed if necessary, to improve homoscedasticity and normality. Differences in anatomical, morphological, and physiological traits between life-history groups (deciduous and evergreen species) were assessed by independent *t*-tests on the mean species values. One-way analysis of variance (ANOVA), followed by *post-hoc* Tukey test ($P < 0.05$), were used to determine the statistical significance of the variation in $g_{\text{leaf-res}}$ components across species. Pearson's linear correlation analyses were used to investigate the relationship between the water leaks through minimum transpiration with the traits that reflect aspects of carbon assimilation and water use among the species. To reduce the dimensionality of the data set and to identify the variables that explained most of the total variation, a principal component analysis (PCA) was used to explore multiple associations among leaf traits that might explain the variability in $g_{\mathrm{leaf\text{-}res}}$ rates both across species and functional groups. All the statistical analyses were performed in R v.3.6.1 (R. Development Core Team, 2018).

In order to predict the impact of the $g_{\mathrm{leaf\text{-}res}}$ variability on the survival of plants under a scenario of water deprivation, we used the *SurEau* model (Martin-StPaul *et al.*, 2017; Cochard *et al.*, 2020), which simulates water transport in the soil-plant-atmosphere continuum, and includes a detailed representation of capacitance in stems and leaf tissues (see Cochard *et al.*, 2020 for detailed information). In this model, tree mortality is assumed to be triggered by hydraulic failure, and a plant is considered dead when its loss 99% of hydraulic conductivity (Martin-StPaul *et al.*, 2017). For the simulations, the time to hydraulic failure (THF), and time to stomatal closure ($T_{\mathrm{gs\text{-}close}}$) were computed based on mean species values of $g_{\mathrm{leaf\text{-}res}}$ and g_{s}, with all other parameters being equal across species (Supporting Information Table S2).

RESULTS

Variability in $g_{\mathrm{leaf\text{-}res}}$ rates across species and its association with cuticle and stomata morphoanatomical properties

Substantial differences in $g_{\mathrm{leaf\text{-}res}}$ (~6 fold) (Table 3) were observed across species. However, although this high variability was associated with leaks arising from both adaxial and abaxial leaf sides (Fig. 2a, b), their relative contribution differed substantially (Fig. 2e). In fact, we found that g_{abaxial} contributed 58% of the total $g_{\mathrm{leaf\text{-}res}}$, whereas $g_{\mathrm{cuticle\text{-}adaxial}}$ contributed 42% (Fig. 2e). This higher permeance of the abaxial leaf side varied largely across species (from 51 to 70%) and had a substantial contribution of the leaks arising from stomata (Table 3 and Supporting Information Table S3). On average, g_{stomata} represented 36% of total g_{adaxial}, but this relative contribution varied substantially across species, with the lowest values observed in *A. aculeata* (13.1%) and the highest in *C. sylvestris* (61.1%) (Fig. 2; Supplementary Information Table 3). As a consequence of the significant impact of g_{stomata} on g_{adaxial}, the water leaks from stomata also represented a considerable fraction of total $g_{\mathrm{leaf\text{-}res}}$ (21%), with the relative contribution across species ranging from 6.6% to 43.6% (Fig. 2; Supporting Information Table S3). This high variability in the relative contribution of g_{stomata} to overall $g_{\mathrm{leaf\text{-}res}}$ (~6 fold) was directly associated with stomatal properties. Across species, $g_{\mathrm{leaf\text{-}res}}$ and g_{stomata} were positively correlated with *SD*, f_{gc}, and g_{wmax}, and negatively correlated with *SS* (Fig. 5; Table 4). However, although between life-history groups the stomatal properties were tightly associated with g_{leaf} and its components (Fig. 5; Table 4), within each group those associations were less evident (Supporting Information Table S4). Within deciduous species, for example, g_{stomata} was positively correlated with g_{wmax} and f_{gc}, whereas for evergreens no significative associations between stomatal properties and leaf water leaks were observed (Supporting Information Table S4).

Despite the large variation observed in cuticle thickness between the adaxial and abaxial leaf sides (Fig. 3d; Table 3), variations in $g_{\mathrm{leaf\text{-}res}}$, $g_{\mathrm{cuti\text{-}adaxial,}}$ and $g_{\mathrm{cuti\text{-}abaxial}}$ were not associated with any of the measured cuticle traits, both across species and within functional groups (Fig. 3; Table 4 and Supporting Information Table S4). However, although cuticle traits were poorly related to the $g_{\mathrm{leaf\text{-}res}}$ variability across species, variations in the thickness of this cellular component were tightly associated with increases in LMA (Table 4).

The variability of water leakiness and traits of cuticle and stomata were also reflected in contrasting life-history strategies (Tables 3 and 4). In general, deciduous species showed higher water leaks, both in the adaxial ($g_{\mathrm{cuti\text{-}adaxial}}$) and abaxial leaf side (g_{abaxial}) (Fig. 2f), thus resulting in higher $g_{\mathrm{leaf\text{-}res}}$ rates, when compared to evergreen species (Fig. 2f; Table 3). A similar pattern was also observed when the water leaks from the abaxial side were decomposed into its main components, with deciduous species presenting higher $g_{\mathrm{cuti\text{-}abaxial}}$ and g_{stomata} rates, in relation to evergreen species (Fig. 2f; Table 3). The higher $g_{\mathrm{leaf\text{-}res}}$ and g_{stomata} rates of deciduous species, by its turn, were tightly associated with their higher *SD*, $f_{\mathrm{gc,}}$ and g_{wmax}, and lower *SS*, in comparison to the evergreen species (Fig. 5; Table 4). However, despite the high variability in stomata traits, significative differences between life-history groups were not found in any of the cuticle properties (Fig. 4; Table 3). Within functional groups, although the leakiness arising from the cuticle were significantly higher than those from stomata, differences in cuticular transpiration between leaf sides were not detected (Fig. 2f; Table 3).

Growth strategies and its implications for carbon assimilation and water loss among species

The Cerrado species differed substantially on their carbon assimilation capacity (*A*) (Table 3), and this difference across species was mainly associated with diffusive aspects, as denoted by the high positive correlation found between *A* with g_s (Fig. 4a). In addition to the physiological regulation of the stomatal movements, represented by g_s, the CO_2 diffusion capacity, and thus *A* rates, among species were also affected by stomatal morphological aspects (Fig. 5; Tables 3, 4 and Supporting Information Table S3). In fact, *A* rates were positively correlated with *SD*, f_{gc}, and

g_{wmax}, and negatively correlated with *SS* (Table 4). The differences in *A* rates were directly related to the growth strategy of the studied species (Fig. 4a; Table 3). Deciduous species showed a fast-growing strategy, which involved physiological, anatomical, and morphological aspects that allowed for high CO_2 diffusion (higher g_s, *SD*, f_{gc} and g_{wmax}, and lower *SS*), resulting in higher *A* rates, but also increased water loss (*E*) (Fig. 5; Tables 3 and 4,). Evergreen species, on the other hand, were characterized by a more conservative growth strategy, represented by lower *A* and *E* rates, due to lower g_s, *SD*, f_{gc} and g_{wmax}, and higher *SS* (Fig. 5; Tables 3 and 4).

The fast-growing strategy of deciduous species, although allowing higher carbon assimilation (*A*), also resulted in higher water leaks ($g_{\mathrm{leaf\text{-}res}}$), when compared to the more conservative strategy of evergreen species (Fig. 5; Table 3). The high positive correlation found between *A* and g_s with $g_{\mathrm{leaf\text{-}res}}$ (Fig. 4; Table 4) represents the base of the trade-off between carbon assimilation and water leaks, which is linked by stomatal properties (Figs. 4 and 5), as denoted by the high positive correlations between *SD*, $f_{\mathrm{gc},}$ and g_{wmax} with *A*, g_s, $g_{\mathrm{leaf\text{-}res}}$, and g_{stomata} (Figs. 4 and 5; Table 4).

The contrasting growth strategy between functional groups was further investigated with a PCA analysis. The first two components explained 73.1% of the total variation in the data (Fig. 6). The first component explained 47% of the total variation and clearly shows that higher carbon assimilation of deciduous species was associated with morphoanatomical adjustments that maximize the CO_2 diffusion into the leaves but, at the same time, result in higher water loss (Figs. 6 and 7). The second component explained an additional 26.1% of the variation and shows that, along this axis, the species were primarily separated by their contrasting investment in cuticle and stomata density and size (Fig. 6).

Water leaks and leaf mortality

Although the water loss through $g_{\mathrm{leaf\text{-}res}}$ represented only a small fraction of the total water loss by transpiration, our modeling approach demonstrated that these small leaks could have a great impact on leaf mortality under drought conditions (Fig. 8). The fast-growing strategy of deciduous species, which was associated with higher $g_{\mathrm{leaf\text{-}res}}$ rates (Figs. 2 and 4; Table 3), resulted in a mean time to leaf hydraulic failure of 51 days (Fig. 8), whereas the more conservative strategy of evergreen species resulted in a substantially longer survival time under the modeled scenario of severe drought stress (78 days) (Fig. 8). Our simulations also showed that contrasting g_s rates significantly impacted the time to stomatal closure ($T_{\text{gs-close}}$) under drought, with deciduous species closing their stomata earlier than evergreens (Fig. 8).

Discussion

Our results provide a new perspective of the main drivers underlying the variability in minimum conductance across plant species from the most diverse Brazilian domain. More specifically, we show that variation in $g_{\text{leaf-res}}$ across species is associated with differential allocation of stomatal cells into the epidermis, as a consequence of their contrasting growth strategies. To the best of our knowledge, this is the first study to report the possible existence of a trade-off between carbon assimilation and water loss by minimum transpiration. In addition, we also show that these water leaks, although representing a small fraction of the total water loss through transpiration, can have a huge impact on the strategies of water use and conservation between life-history groups, with possible negative impacts on leaf survival, especially under drought conditions.

How variations in the relative investment in cuticle and stomata affect the $g_{\text{leaf-res}}$ rates across species?

Our results demonstrate that, although both $g_{\text{cuti-adaxial}}$ and g_{abaxial} significantly explained the high $g_{\text{leaf-res}}$ variability across the studied species (Fig. 2a, b), their relative contribution differed substantially. In fact, the leaf abaxial side had a mean contribution of 58% of the total minimum transpiration across species (Fig 2e), although in some cases this relative contribution was substantially higher (70%) (Supporting Information Table S3). This result complements the yet scarce, but growing body of evidence suggesting that the overall minimum transpiration arises from heterogeneous water leaks between leaf sides (Šantrůček *et al.*, 2004; Brodribb *et al.*, 2014). In addition, as all the studied species are hypostomatous, we also expected that this higher permeance of the abaxial side of the leaves would be strongly related to stomatal properties, especially their density and size. More specifically, considering that stomata pores can be particularly leaky (Kerstiens, 1996a; Šantrůček *et al.*, 2004), even when they were supposed to be closed (e.g. drought conditions), the increase in stomatal density (*SD*) would result in increased g_{stomata} and g_{abaxial} rates due to the higher proportion of potentially leaky stomatal pores covering the leaf epidermis. This hypothesis is supported by our results since the species with higher *SD* were those reporting the highest g_{abaxial} and g_{stomata} values (Table 4). In fact, variations in g_{stomata}, as well as the relative contribution of this trait to overall $g_{\text{leaf-res}}$, were positively associated with increases in *SD* (Table 4; Supporting Information Fig. S4). The substantial divergence in *SD* across species, in its turn, was tightly related to reductions in *SS* and *p* (Table 3; Supporting Information Fig. S4), a result that reflects the already well-documented constraints of epidermis space allocation (Franks *et al.*, 2009; de Boer *et al.*, 2016). In this regard, although the increase in *SD* would lead to reductions in *SS* and *p* of individual guard cells, the overall result is an inevitable increase in relative pore length, leading to higher water leaks through the stomatal pore ($g_{\text{stomata-pore}}$, Fig. 1) and, consequently, higher g_{stomata} and g_{abaxial} in the species that followed this strategy (Supporting Information Fig. S4)

In addition to the leaks that arise from the stomatal pore, the higher permeance of the abaxial leaf surface can also be related to the lower resistance to water flux from the guard cells (Schuster *et al.*, 2017). In fact, it was already shown that the cuticle layer that covers the guard cells lacks important chemical components, which may increase its permeance (Bargel *et al.*, 2004; Duursma *et al.*, 2019). Accordingly, a detailed study on *Hedera helix* demonstrated that a significative proportion of the water flux from the abaxial surface of the leaves occurs through the non-porous surface (Šantrůček *et al.*, 2004), another indicator of the higher permeance of guard cells. If guard cells present higher water permeance, it could be expected that increases in the allocation of the epidermis to stomata should result in higher $g_{\text{leaf-res}}$ rates. Our results confirm this hypothesis since we found significative positive correlations between f_{gc}, a trait which integrates variations in guard cell area and stomatal density, with g_{stomata} and $g_{\text{leaf-res}}$ (Fig. 5; Table 4). Thus, considering that the abaxial leaf side had a significative higher contribution to the overall minimum transpiration (Fig. 2e,f), and assuming that the leaks on this surface were associated with incomplete stomatal closure and/or lower resistance to water flux from the guard cells, the high $g_{\text{leaf-res}}$ variability found among Cerrado species (~6 fold) was probably a reflection of their contrasting allocation of epidermis to stomata, as a result of variation in *SD* and *SS* (Fig. 5; Tables 3 and 4). When taken together, these results reinforce the "leaky stomata" hypothesis (Kerstiens, 1996a; Šantrůček *et al.*, 2004; Duursma *et al.*, 2019), and suggest that the ecological strategies that result in differential distribution of stomata in the epidermis can have a significative impact on the overall $g_{\text{leaf-res}}$ rates across species. In fact, although for some species g_{stomata} represented just a small fraction of total $g_{\text{leaf-res}}$ (6.6%), for others those stomatal water leaks accounted for almost half of total residual water loss (43.6%) (Table 4, Supporting Information Table S3). In both cases, variations in g_{stomata}, and its effects on $g_{\text{leaf-res}}$, were tightly associated with differences in stomatal properties (Table 4; Supporting Information Fig. S4), even when differences in the cuticle conductance from the abaxial leaf sides were considered (Supporting Information Figs. S2 and S3).

Given the high contribution of cuticular transpiration from both leaf sides to the overall variation in $g_{\text{leaf-res}}$ among species, we also expected that increases in the relative investment in cuticle would be associated with reductions in $g_{\text{cuti-adaxial}}$ and $g_{\text{cuti-abaxial}}$ rates, thus leading to lower $g_{\text{leaf-res}}$ values. However, contrary to our hypothesis, although we have found substantial differences in cuticle thickness in both adaxial and abaxial sides among species (Fig. 3d; Table 3), the expected negative correlation between cuticle thickness with $g_{\text{cuti-adaxial}}$, $g_{\text{cuti-abaxial,}}$ and $g_{\text{leaf-res}}$ was not observed (Fig. 3d; Table 3). If the cuticle represents the main barrier against water loss (Schuster *et al.*, 2017; Bueno *et al.*, 2019), how could the increase in its thickness not be associated with reductions in minimal transpiration? The most likely answer to this question resides in the fact that the main diffusion barrier of the cuticle consists of a thin layer of wax (the limit skin), deposited at or near the outer surface of this membrane (Schreiber, 2001). This helps to explain why variations in $g_{\text{leaf-res}}$ are better explained by differences in cuticle composition (Bargel *et al.*, 2004; Bueno *et al.*, 2019) rather than its thickness (Jetter *et al.*, 2016). Considering that increases in cuticle thickness were not associated with a reduction in $g_{\text{leaf-res}}$ rates, what could explain the substantial differences in the relative investment of this structure among Cerrado species? The high positive correlations found between cuticle thickness with LMA (Table 4) is a good indication of other possible ecological functions that may be fulfilled by the cuticle. As LMA is a trait that reflects the trade-off between carbon gain and longevity (Poorter *et al.*, 2009; John *et al.*, 2017), the differences in cuticle thickness among species may reflect their contrasting carbon investment in leaf construction and protection against biotic and abiotic stressors.

What are the benefits and costs associated with high $g_{\text{leaf-res}}$ rates? Trade-offs underlying the $g_{\text{leaf-res}}$ variability among species with contrasting growth strategies

We hypothesized that contrasting ecological strategies, which result in a differential stomata distribution across the leaf epidermis, would also reflect the $g_{\text{leaf-res}}$ variability between life-history groups. This hypothesis also seems to be confirmed since the large variation observed in $g_{\text{leaf-res}}$ rates between deciduous and evergreen species (~2 fold) was tightly related to the substantial differences found in their stomata size and distribution (Fig. 5; Tables 3 and 4). In addition, the differences in stomata properties among life-history groups also reflected their contrasting growth strategies, as denoted by the marked differences in their *A* rates (Fig. 4; Table

3). Thus, as stomata morphology had a direct impact on both CO_2 diffusion (g_{wmax} and g_s) and water leaks ($g_{leaf\text{-}res}$), we predicted the existence of a trade-off between carbon assimilation and water loss through minimum transpiration. The positive correlations found between A and $g_{leaf\text{-}res}$ with g_s and g_{wmax} (Fig. 4, Table 4) confirm this hypothesis and suggest that variations in $g_{leaf\text{-}res}$ between functional groups arise as a consequence of the anatomical and morphological adjustments associated with their contrasting growth strategies (Figs. 6 and 7).

In order to maximize carbon acquisition through their short growing season, deciduous species tended to maximize photosynthesis during the wet period, at the expense of higher water loss through transpiration; whereas evergreen species showed a more conservative strategy of carbon assimilation and water use (Fig. 6). Thus, considering that all measurements were made during the wet season and that biochemical limitation to photosynthesis is usually triggered by extreme drought events (Flexas *et al.*, 2009; Tosens *et al.*, 2016), the highly positive correlations found between A and g_s suggest that higher photosynthetic potential of deciduous species probably involved a high CO_2 diffusion capacity. Although g_s rates can be affected within a few minutes, through dynamic alterations in stomatal pore aperture (Drake *et al.*, 2013) and/or by changes in mesophyll conductance (Flexas *et al.*, 2007), the physiological limits of CO_2 diffusion (g_{wmax}) are set morphoanatomically, through alterations in *SS* and *SD* (Franks & Beerling, 2009; Haworth *et al.*, 2018; Bertolino *et al.*, 2019). The highly positive correlations found between g_s with g_{wmax} (Fig. 5, Table 4) reinforce the role of anatomical and morphological adjustments in determining the rates of CO_2 diffusion and suggest that differences in photosynthetic potential among contrasting life-history strategies were mainly determined by different combinations of *SS* and *SD* (Figs. 5 and 6; Tables 3 and 4). In fact, the higher A rates of deciduous species, when compared to evergreen ones (Fig. 4; Table 3), were tightly associated with the investment in smaller and more numerous stomata, which possibly resulted in increased CO_2 diffusion capacity, as evidenced by their higher values of g_s and g_{wmax} (Figs. 4, 5 and 6; Tables 3 and 4). However, although this strategy allows deciduous species to achieve higher growth potential during the rainy season (Fig. 6), under drought conditions, the investment in small and numerous stomata would probably increase leaf water leaks. In fact, given the high contribution of stomata leakiness to the overall variation in minimum conductance (Fig. 2), the increase in water leaks in the abaxial side, as a result of higher *SD* and lower *SS*, will inevitably lead to higher $g_{stomata}$, and thus $g_{leaf\text{-}res}$ rates (Fig. 2; Tables 3 and 4). From this perspective, the leaf shedding of deciduous species in the dry season probably acts as a safety valve to avoid the extensive water loss due to high $g_{leaf\text{-}res}$ rates associated with their fast-growing strategy (discussed below). On the other hand, the more conservative growth strategy of evergreen species (Fig. 6), resulting from greater *SS* and lower *SD*, has as one of the main benefits the reduced water loss during the Cerrado drought season, at the expense of reduced *A* rates driven by lower g_s and g_{wmax} (Figs. 2, 5, 6 and 7; Tables 3 and 4). However, it is important to note that, although our results had clearly demonstrated the role of stomata leakiness in determining the overall $g_{leaf\text{-}res}$ variation in Cerrado species the contribution of water loss through the cuticle, especially in the adaxial side, cannot be neglected. In this way, more studies are needed to further understand how the adjustments in stomata size and density might be tuned to variability in cuticle properties, more specifically its chemical composition.

How broad the trade-off between carbon assimilation and water loss by minimum transpiration can be?

Although our results provide strong evidence of the coordination between differential stomatal allocation into the epidermis with $g_{leaf\text{-}res}$ variation across Cerrado species with contrasting leaf habits (Figs. 5, 6 and 7; Table 3 and 4; Supporting Information Fig S4), those associations become less clear when the groups were analyzed separately (Supporting Information Table S4). These results might suggest that the coordination between stomatal properties (e.g. *SD,* $f_{gc,}$ and g_{wmax}) with leaf water leaks probably are more evident when a broad spectrum of species, encompassing a wide variation in stomatal size and density, are analyzed, as in the case of the evergreen and deciduous species investigated in this study (Table 3). However, this hypothesis seems to be refuted by the evidence showing that $g_{leaf\text{-}res}$ can be extremely responsive to even small variations in *SD*, as already reported for *Sorghum* genotypes (Muchow & Sinclair, 1989), and recently observed within *Coffea canephora* cultivars (unpublished results, Supporting Information Fig. S5). Further evidence of the role of stomatal leakiness in driving $g_{leaf\text{-}res}$ rates was also observed in *C. pachystachya* plants exposed to extreme weather conditions (drought and heat stresses), in which variations in *SD*, due to leaf acclimation, were tightly coordinated with changes in $g_{leaf\text{-}res}$ and g_s (unpublished results, Supporting Information Fig. S5). In this way, although the weak trends observed within functional groups of Cerrado species needs to be further investigated, the highly positive correlations found between g_s and $g_{leaf\text{-}res}$ with *SD*, and between $g_{leaf\text{-}res}$ with g_s, both within cultivars and under contrasting abiotic stresses, suggest that the trade-off between carbon assimilation and water loss by minimum transpiration seems to operate across a wide range of plant species and to be responsive to different environmental conditions.

Consequences of the $g_{\text{leaf-res}}$ variability across species: implications for strategies of water use and conservation

Our results demonstrate that the contrasting growth strategies between deciduous and evergreen species had a direct impact on their $g_{\text{leaf-res}}$ rates (Figs. 6 and 7, Tables 3 and 4). However, considering that the water loss from minimum transpiration found in the present study represented just a small fraction of the total water loss through transpiration, what could be the real impact of those small leaks to the overall water balance of the studied species? The ecological implications of the variability in $g_{\text{leaf-res}}$ rates are fully appreciated under drought conditions. As the soil dries, the tension in the xylem vessels tends to increase considerably, which may reduce the stability of the water column and, ultimately, lead to cavitation (breakage of the water column) (Schuldt *et al.*, 2016; Hochberg *et al.*, 2019). As a consequence, cavitation can lead to extensive hydraulic failure, reducing a plant's ability to replenish the water lost through transpiration and resulting in extreme desiccation and death (Choat *et al.*, 2012; Mitchell *et al.*, 2013; Hartmann *et al.*, 2018). In this way, the ability to avoid excessive water loss significantly reduce the drop in the water potential, and thus postpone the time to hydraulic failure (Mcculloh *et al.*, 2014; Anderegg *et al.*, 2019). Our modelling approach demonstrates that the main components of the trade-off discussed above have distinct roles in the intricate dynamics of plant dehydration under drought conditions, with g_s determining the time to stomatal closure and $g_{\text{leaf-res}}$ the time to hydraulic failure (Fig. 8). For instance, the higher carbon assimilation rates of fast-growing species (deciduous), which required higher g_s, lead to high transpiration and faster depletion of soil and plant tissues water reserves, triggering an earlier stomatal closure, when compared to species with more a conservative water use strategy (evergreens) (Fig. 8). Although this earlier stomatal closure has the potential to reduce the drop in water potential and thus postpone the THF, the anatomical and morphological adjustments necessary to allow higher CO_2 influx under well watered conditions inevitably lead to higher water loss through minimum transpiration under drought, thus resulting in lower THF (Fig. 8). In this regard, our simulations show that although small, the water leaks from minimum transpiration can have a great impact on THF and suggest that, in addition to earlier stomatal closure (Martin-StPaul *et al.*, 2017), the survival under drought conditions also rely on the ability to minimize those water leaks.

Although our simulations suggest that the higher $g_{\text{leaf-res}}$ rates of deciduous species would make them more vulnerable to drought, other important physiological aspects must be considered when interpreting these results. It is not clear, for example, if deciduous species from the Brazilian Cerrado present the hydraulic segmentation strategy, in which organs that represent a lower carbon investment (e.g. leaves and small roots) are more vulnerable to cavitation than more basal organs (e.g. branches and trunks) (Zimmermann, 1983; Tyree & Ewers, 1991). Several studies already showed that the cavitation of leaves can act as a hydraulic valve, protecting the spread of embolism to the trunks (Chen *et al.*, 2009; Bucci *et al.*, 2012, 2013, Zhu *et al.*, 2016). From this perspective, it is possible that deciduous species shed their leaves under drought conditions as a strategy to avoid excessive water loss due to their higher $g_{\text{leaf-res}}$ rates. On the other hand, a lack of hydraulic segmentation between organs has been reported for other several species (Skelton *et al.*, 2017; Klepsch *et al.*, 2018; Smith-Martin *et al.*, 2020), and thus alternative mechanisms might be involved in protecting leaf and stem xylem against cavitation, such as changes in leaf outside xylem pathways (Scoffoni & Sack, 2017). Unfortunately, due to the lack of information regarding the vulnerability to drought for the studied species, these hypotheses cannot be confirmed.

Conclusions

The results obtained in the present study provide a new perspective of the main drivers of $g_{\text{leaf-res}}$ variability across species with contrasting growth strategies. We show that water loss through stomata leakiness can have a significative impact in determining the overall $g_{\text{leaf-res}}$ since for some species g_{stomata} accounted for almost half of total residual water loss. In addition, our results provide strong evidence that the $g_{\text{leaf-res}}$ variability across species and functional groups arise as a result of a trade-off between carbon assimilation and water loss, as suggested by the highly positive association found between $g_{\text{leaf-res}}$ with A, and that this variability may have a huge impact on the time to hydraulic failure, and thus in the survival time under drought conditions. Overall, the present study increases the knowledge regarding the water leaks after stomatal closure of the plants that compose one of the largest and most diverse Brazilian biomes.

Acknowledgments

This study was funded by Conselho Nacional de Desenvolvimento Científico e Tecnológico (CNPq) (grants nº 207920/2017-6 and 432264/2018-3 to P.E.M-S; and 408083/2016-6 to FSF), Agence Nationale de la Recherche (ANR) (grant nº 18-CE20-0005 to H.C. and J.M.T-R), and by the Instituto Federal Goiano.

Author contribution

RM, LL-L, FSF, PEM-S, and HC designed the experiment. RM, LL-L, RDFBA, and LFS performed sample collection. RM, LL-L, RBFBA, and LFS performed the physiological analysis. SCVF, FSF, and RM processed and photographed the morphoanatomical material. HC performed the model simulations. PEM-S wrote the manuscript with contributions from HC, JMT-R, FGS, SCVF, and FSF. RM and LL-L contributed equally to this work.

References

Anderegg WRL. **2015**. Spatial and temporal variation in plant hydraulic traits and their relevance for climate change impacts on vegetation. *New Phytologist* **205:** 1008–1014.

Anderegg WRL, Anderegg LDL, Kerr KL, Trugman AT. **2019**. Widespread drought-induced tree mortality at dry range edges indicates climate stress exceeds species' compensating mechanisms. *Global Change Biology*: gcb.14771.

Bacelar EA, Correia CM, Moutinho-Pereira JM, Gonçalves BC, Lopes JI, Torres-Pereira JMG. **2004**. Sclerophylly and leaf anatomical traits of five field-grown olive cultivars growing under drought conditions. *Tree Physiology* **24**: 233–239.

Bargel H, Barthlott W, Koch K, Schreiber L, Neinhuis C. 2004. Plant cuticles: multifunctional interfaces between plant and environment. In The evolution of plant physiology. Academic Press. pp. 171-III.

Bertolino LT, Caine RS, Gray JE. **2019**. Impact of stomatal density and morphology on water-use efficiency in a changing world. *Frontiers in Plant Science* **10**:225.

Billon LM, Blackman CJ, Cochard H, Badel E, Hitmi A, Cartailler J, Souchal R. **2020**. The DroughtBox : A new tool for phenotyping residual branch conductance and its temperature dependence during drought. *Plant, Cell and Environment* **2020:** 1–11.

de Boer HJ, Price CA, Wagner-Cremer F, Dekker SC, Franks PJ, Veneklaas EJ. **2016**. Optimal allocation of leaf epidermal area for gas exchange. *New Phytologist* **210**: 1219–1228.

Brodribb TJ, Mcadam SAM, Jordan GJ, Martins SC V. **2014**. Conifer species adapt to low-rainfall climates by following one of two divergent pathways. *Proceedings of the National Academy of Sciences of the United States of America* **111:** 14489-14493.

Bucci SJ, Scholz FG, Campanello PI, Montti L, Jimenez-Castillo M, Rockwell FA, Manna LL, Guerra P, Bernal PL, Troncoso O, Enricci J, Holbrook MN, Goldstein G. 2012.

Hydraulic differences along the water transport system of South American Nothofagus species: do leaves protect the stem functionality? *Tree Physiology* **32**: 880–893.

Bucci SJ, Scholz FG, Peschiutta ML, Arias NS, Meinzer FC, Goldstein G. **2013**. The stem xylem of Patagonian shrubs operates far from the point of catastrophic dysfunction and is additionally protected from drought-induced embolism by leaves and roots. *Plant, Cell and Environment* **36**: 2163–2174.

Bueno A, Alfarhan A, Arand K, Burghardt M, Deininger AC, Hedrich R, Leide J, Seufert P, Staiger S, Riederer M. **2019**. Effects of temperature on the cuticular transpiration barrier of two desert plants with water-spender and water-saver strategies. *Journal of experimental botany* **70**: 1613–1625.

Chen JW, Zhang Q, Li XS, Cao KF. 2009. Independence of stem and leaf hydraulic traits in six Euphorbiaceae tree species with constrasting leaf phenology. *Planta* **230**: 459-468.

Choat B, Jansen S, Brodibb TJ, Cochard H, Delzon S, Bhaskar R, Bucci SJ, Feild taylor s, Gleason SM, Al E. **2012**. Global convergence in the vulnerability of forest to drought. *Nature* **491**: 752–755.

Cochard H. **2019**. A new mechanism for tree mortality due to drought and heatwaves. *bioRxiv*. doi: 10.1101/531632

Cochard H, Pimont F, Ruffault J, Martin-stpaul N. **2020**. SurEau . c : a mechanistic model of plant water relations under extreme drought. *bioRxid*. doi: 10.1101/2020.05.10.086678

Drake PL, Froend RH, Franks PJ. **2013**. Smaller, faster stomata: Scaling of stomatal size, rate of response, and stomatal conductance. *Journal of Experimental Botany* **64**: 495–505.

Duursma RA, Blackman CJ, Lopéz R, Martin-StPaul NK, Cochard H, Medlyn BE. **2019**. On the minimum leaf conductance: its role in models of plant water use, and ecological and environmental controls. *New Phytologist* **221**: 693–705.

Flexas J, Barón M, Bota J, Ducruet JM, Gallé A, Galmés J, Jiménez M, Pou A, Ribas-Carbó M, Sajnani C, *et al.* **2009**. Photosynthesis limitations during water stress acclimation and recovery in the drought-adapted *Vitis* hybrid Richter-110 (*V. berlandieri*×*V. rupestris*). *Journal of Experimental Botany* **60**: 2361–2377.

Flexas J, Diaz-espejo A, Galmés J, Kaldenhoff R, Medrano H. **2007**. Rapid variations of mesophyll conductance in response to changes in CO_2 concentration around leaves. *Plant, Cell and Environment* **30**: 1284–1298.

Franco AC, Bustamante M, Caldas LS, Goldstein G, Meinzer FC, Kozovits AR, Rundel P,

Coradin VTR. **2005**. Leaf functional traits of Neotropical savanna trees in relation to seasonal water deficit. *Trees - Structure and Function* **19**: 326–335.

Franks PJ, Beerling DJ. **2009**. Maximum stomatal conductance driven by CO2 effects on stomatal size and density over geological time. *Proceedings of the National Academy of Sciences of the United States of America* **106**: 10343–10347.

Franks PJ, Drake PL, Beerling DJ. **2009**. Plasticity in maximum stomatal conductance constrained by negative correlation between stomatal size and density: An analysis using *Eucalyptus globulus*. *Plant, Cell and Environment* **32**: 1737–1748.

Galmés J, Ochogavía JM, Gago J, Roldán EJ, Cifre J, Conesa MÀ. **2013**. Leaf responses to drought stress in Mediterranean accessions of *Solanum lycopersicum*: Anatomical adaptations in relation to gas exchange parameters. *Plant, Cell and Environment* **36**: 920–935.

Gleason SM, Blackman CJ, Cook AM, Laws CA, Westoby M. **2014**. Whole-plant capacitance, embolism resistance and slow transpiration rates all contribute to longer desiccation times in woody angiosperms from arid and wet habitats. *Tree Physiology* **34**: 275–284.

Gotsch SG, Powers JS, Lerdau MT. **2010**. Leaf traits and water relations of 12 evergreen species in Costa Rican wet and dry forests: Patterns of intra-specific variation across forests and seasons. *Plant Ecology* **211**: 133–146.

Hartmann H, Moura CF, Anderegg WRL, Ruehr NK, Salmon Y, Allen CD, Arndt SK, Breshears DD, Davi H, Galbraith D, *et al.* **2018**. Research frontiers for improving our understanding of drought-induced tree and forest mortality. *New Phytologist* **218**: 15–28.

Haworth M, Scutt CP, Douthe C, Marino G, Gomes MTG, Loreto F, Flexas J, Centritto M. **2018**. Allocation of the epidermis to stomata relates to stomatal physiological control: Stomatal factors involved in the evolutionary diversification of the angiosperms and development of amphistomaty. *Environmental and Experimental Botany* **151**: 55–63.

Hochberg U, Ponomarenko A, Zhang YJ, Rockwell FE, Holbrook NM. **2019**. Visualizing embolism propagation in gas-injected leaves. *Plant Physiology* **180**: 874–881.

Jetter R, Riederer M. **2016**. Localization of the transpiration barrier in the epi- and intracuticular waxes of eight plant species: Water transport resistances are associated with fatty acyl rather than alicyclic components. *Plant Physiology* **170**: 921–934.

John GP, Scoffoni C, Buckley TN, Villar R, Poorter H, Sack L. **2017**. The anatomical and compositional basis of leaf mass per area. *Ecology Letters* **20**: 412–425.

Kerstiens G. **1996a**. Cuticular water permeability and its physiological significance. *Journal of*

Experimental Botany **47**: 1813–1832.

Kerstiens G. **1996b**. Signalling across the divide: A wider perspective of cuticular structure-function relationships. *Trends in Plant Science* **1**: 125–129.

Klein T, Randin C, Korner C. 2015. Water availability predicts forest canopy height at the global scale. *Ecology Letters* 18: 1311-1320.

Klepsch M, Zhang Y, Kotowska MM, Lamarque LJ, Nolf M, Cao K, Jansen S. **2018**. Is xylem of angiosperm leaves less resistant to embolism than branches? Insights from microCT, hydraulics, and anatomy. *Journal of Experimental Botany* **69**: 5611–5623.

Loram-lourenço L, Farnese F, Menezes-silva PE. **2020**. A Structure Shaped by Fire , but Also Water : Ecological Consequences of the Variability in Bark Properties Across 31 Species From the Brazilian Cerrado A Structure Shaped by Fire , but Also Water : Ecological Consequences of the Variability in Bark Properties Across 31 Species From the Brazilian Cerrado. *Frontiers in Plant Science* **10**:1718.

Markesteijn L, Poorter L, Bongers F, Paz H, Sack L. **2011**. Hydraulics and life history of tropical dry forest tree species: Coordination of species' drought and shade tolerance. *New Phytologist* **191**: 480–495.

Martin-StPaul N, Delzon S, Cochard H. **2017**. Plant resistance to drought depends on timely stomatal closure. *Ecology Letters* **20**: 1437–1447.

Mcadam SAM, Brodribb TJ. **2012**. Stomatal innovation and the rise of seed plants. *Ecology Letters* **15**: 1–8.

Mcculloh KA, Johnson DM, Meinzer FC, Woodruff DR. **2014**. The dynamic pipeline: Hydraulic capacitance and xylem hydraulic safety in four tall conifer species. *Plant, Cell and Environment* **37**: 1171–1183.

Mitchell PJ, O'Grady AP, Tissue DT, White DA, Ottenschlaeger ML, Pinkard EA. **2013**. Drought response strategies define the relative contributions of hydraulic dysfunction and carbohydrate depletion during tree mortality. *New Phytologist* **197**: 862–872.

Muchow RC, Sinclair TR. 1989. Epidermal conductance, stomatal density and stomatal size among genotypes of Sorghum bicolor (L.) Moench. *Plant, Cell and Environment* **12**: 425-431.

Percy RW, Schulze ED, Zimmermann R. 2000. Measurement of transpiration and leaf conductance. In Plant Physiological Ecology: Field Methods and Instrumentation (eds RW Percy, JR Ehlenringer, HA Mooney & PW Rundel), pp. 137-160. Kluwer Academic, Dordrecht, The Netherlands.

Poorter H, Niinemets U, Poorter L, Wright IJ, Villar R. **2009**. Causes and consequences of variation in leaf mass per area (LMA):a meta-analysis. *New phytologist* **182**: 565–588.

R Core Team. 2015. R: A language and environment for statistical computing. R Foundation for Statistical Computing, Vienna, Austria.

Richardson A, Wojciechowski T, Franke R, Schreiber L, Kerstiens G, Jarvis M, Fricke W. **2007**. Cuticular permeance in relation to wax and cutin development along the growing barley (*Hordeum vulgare*) leaf. *Planta* **225**: 1471–1481.

Rossatto DR, Franco AC. **2017**. Expanding our understanding of leaf functional syndromes in savanna systems: the role of plant growth form. *Oecologia* **183**: 953–962.

Sack L, Cowan PD, Jaikumar N, Holbrook NM. **2003**. The 'hydrology' of leaves: Co-ordination of structure and function in temperate woody species. *Plant, Cell and Environment* **26**: 1343–1356.

Šantrůček J, Šimánová E, Karbulková J, Šimková M, Schreiber L. **2004**. A new technique for measurement of water permeability of stomatous cuticular membranes isolated from *Hedera helix* leaves. *Journal of Experimental Botany* **55**: 1411–1422.

Schreiber L. **2001**. Effect of temperature on cuticular transpiration of isolated cuticular membranes and leaf discs. *Journal of Experimental Botany* **52**: 1893–1900.

Schuldt B, Knutzen F, Delzon S, Jansen S, Müller-Haubold H, Burlett R, Clough Y, Leuschner C. **2016**. How adaptable is the hydraulic system of European beech in the face of climate change-related precipitation reduction? *New Phytologist* **210**: 443–458.

Schuster AC, Burghardt M, Riederer M. **2017**. The ecophysiology of leaf cuticular transpiration: are cuticular water permeabilities adapted to ecological conditions? *Journal of experimental botany* **68**: 5271–5279.

Scoffoni C, Sack L. **2017**. The causes and consequences of leaf hydraulic decline with dehydration. *Journal of Experimental Botany* **68**: 4479–4496.

Skelton R, Brodribb T, Choat B. **2017**. Casting light on xylem vulnerability in an herbaceous species reveals a lack of segmentation. *New Phytologist* **214**: 561-569.

Slavic B. 1974. Methods of studying plant water relations. Berlin: Springer.

Smith-Martin CM, Skelton R, Johnson KM, Lucani C. **2020**. Lack of vulnerability segmentation among woody species in a diverse dry sclerophyll woodland community. *Functional Ecology* **34**: 777-787.

Strassburg BBN, Brooks T, Feltran-Barbieri R, Iribarrem A, Crouzeilles R, Loyola R,

Latawiec AE, Oliveira Filho FJB, Scaramuzza CA de M, Scarano FR, *et al.* 2017. Moment of truth for the Cerrado hotspot. *Nature Ecology & Evolution* **1**: 0099.

Tosens T, Nishida K, Gago J, Coopman RE, Cabrera HM, Carriquí M, Laanisto L, Morales L, Nadal M, Rojas R, *et al.* 2016. The photosynthetic capacity in 35 ferns and fern allies: Mesophyll CO_2 diffusion as a key trait. *New Phytologist* **209**: 1576–1590.

Trueba S, Pouteau R, Lens F, Feild TS, Isnard S, Olson ME, Delzon S. **2017**. Vulnerability to xylem embolism as a major correlate of the environmental distribution of rain forest species on a tropical island. *Plant Cell and Environment* **40**: 277–289.

Tyree MT, Ewers FW. 1991. The hydraulic architecture of trees and other woody plants. *New Phytologist*. 119: 345-360.

Villar R, de la Riva EG, Ubera JL, Olmo M, Poorter H. **2016**. Leaf mass per area (LMA) and its relationship with leaf structure and anatomy in 34 Mediterranean woody species along a water availability gradient. *Plos One* **11**: e0148788.

Xiong D, Flexas J, Yu T, Peng S, Huang J. **2016**. Leaf anatomy mediates coordination of leaf hydraulic conductance and mesophyll conductance to CO_2 in *Oryza*. *New Phytologist* **213**: 572-583.

Zimmermann MH. 1983. Xylem Structure and the Ascent of Sap. Springer-Verlag, Berlin, Germany.

Zhu S-D, Liu H, Xu Q-Y, Cao K-F, Qing Y. 2016. Are leaves more vulnerable to cavitation than branches? *Functional Ecology* **30:** 1740-1744.

Supporting information

Fig. S1. Transverse section of *Himatanthus obovatus* leaf highlighting the cuticle structure.

Fig. S2. Sensitive analysis showing the impact of the variation in cuticular conductance of the abaxial leaf side ($g_{\text{cuti-abaxial}}$) on key components of the leaf minimum conductance ($g_{\text{leaf-res}}$).

Fig. S3. Relationships between variable minimum conductance of stomatal cells (g_{stomata}), due to changes in the cuticular conductance of the abaxial leaf side ($g_{\mathrm{cuti\text{-}abaxial}}$), with stomatal morphoanatomical traits.

Fig. S4. Variation in stomatal density and size and its impacts on the water leaks from the abaxial leaf side.

Fig. S5. Trade-offs between carbon assimilation and water loss through minimum conductance within cultivars of *Coffea canephora*, and in *Cecropia pachystachya* plants exposed to contrasting abiotic stresses.

Methods S1. Detailed description of the determination of leaf minimum water conductance ($g_{\mathrm{leaf\text{-}res}}$) and its main components

Table S1. Mean values of relative humidity (RH) and temperature (T), and their respective variation, during the measurements of leaf minimal conductance ($g_{\mathrm{leaf\text{-}res}}$) for 30 species from the Brazilian Cerrado.

Table S2. Physiological and environmental inputs for the simulation of the influence of variation in minimum conductance on the time to stomatal closure and time to hydraulic failure.

Table S3. Diffusive and morphoanatomical traits for 30 species from Brazilian Cerrado.

Table S4. Relationships between diffusive and morphoanatomical traits within deciduous and evergreen species from Brazilian Cerrado

Table 1. List of the studied species and their leaf habit.

Species	Family	Leaf habit
Acosmium subelegans	Fabaceae	Deciduous
Acrocomia aculeata	Arecaceae	Evergreen
Anacardium humile	Anacardiaceae	Evergreen
Arrabidaea brachypoda	Bignoniaceae	Deciduous
Bauhinia curvula	Fabaceae	Deciduous
Bowdichia virgilioides	Fabaceae	Deciduous
Brosimum gaudichaudii	Moraceae	Deciduous
Butia archeri	Arecaceae	Evergreen
Byrsonima basiloba	Malpighiaceace	Deciduous
Byrsonima intermedia	Malpighiaceace	Evergreen
Campomanesia pubescens	Myrtaceae	Deciduous
Cardiopetalum calophyllum	Annonaceae	Evergreen
Casearia sylvestris	Flacourtiaceae	Deciduous
Cecropia pachystachya	Urticaceae	Evergreen
Chrysophyllum marginatum	Sapotaceae	Evergreen
Cochlospermum regium	Cochlospermaceae	Deciduous
Curatella americana	Dilleniaceae	Deciduous
Diospyros hispida	Ebenaceae	Deciduous
Dipteryx alata	Fabaceae	Evergreen
Genipa americana	Rubiaceae	Evergreen
Handroanthus ochraceae	Bignoniaceae	Deciduous
Himatanthus obovatus	Apocynaceae	Deciduous
Hymenaea stilbocarpa	Fabaceae	Deciduous
Matayba guianensis	Sapindaceae	Deciduous
Protium ovatum	Burseraceae	Deciduous
Qualea grandiflora	Vochysiaceae	Deciduous
Roupala montana	Proteaceae	Evergreen
Solanum lycocarpum	Solanaceae	Deciduous
Syagrus oleracea	Arecaceae	Evergreen
Terminalia argentea	Combretaceae	Deciduous

Table 2. Abbreviations of the measured traits with units

Abbreviation	Trait	Unit
A	Net carbon assimilation	$\mu mol\ CO_2\ m^{-2}\ s^{-1}$
g_{s}	Stomatal conductance	$mmol\ H_2O\ m^{-2}\ s^{-1}$
E	Leaf transpiration	$mol\ H_2O\ m^{-2}\ s^{-2}$
$g_{\text{leaf-res}}$	Leaf minimum conductance	$mmol\ H_2O\ m^{-2}\ s^{-1}$
$g_{\text{cuti-adaxial}}$	Cuticular conductance of the adaxial leaf side	$mmol\ H_2O\ m^{-2}\ s^{-1}$
g_{abaxial}	Conductance of the abaxial leaf side	$mmol\ H_2O\ m^{-2}\ s^{-1}$
$g_{\text{cuti-abaxial}}$	Cuticular conductance of the abaxial leaf side	$mmol\ H_2O\ m^{-2}\ s^{-1}$
g_{stomata}	Conductance of guard cells and stomata pore	$mmol\ H_2O\ m^{-2}\ s^{-1}$
SS	Stomata size	μm^2
SD	Stomata density	$stomata\ mm^{-2}$
fgc	Fraction of epidermis allocated to stomata	%
g_{wmax}	Theoretical maximum stomatal conductance	$mol\ H_2O\ m^{-2}\ s^{-1}$
LMA	Leaf mass area	$g\ m^{-2}$
CT_{adaxial}	Cuticle thickness of the adaxial leaf side	µm
CT_{abaxial}	Cuticle thickness of the abaxial leaf side	µm
CT_{total}	Total cuticle thickness	µm
$T_{\text{gs-close}}$	Time to stomatal closure	days
THF	Time to hydraulic failure	days

Table 3. Variation in diffusive and morphoanatomical traits among species and functional groups (deciduous (*n* = 19) and evergreen (*n* = 11) species) of plants from Brazilian Cerrado.

	Species				Deciduous	Evergreen	*t*- test	
Trait	Min	Max	Mean ± SE	Ratio	Mean ± SE	Mean ± SE	*t*	*P*
A	10.4	24.8	16.2 (0.73)	2.38	18.0 (0.86)	13.2 (0.74)	3.94	***
g_s	165	586	366 (23.3)	3.55	430 (22.3)	255 (28.4)	5.33	***
E	2.92	9.33	5.74 (0.31)	3.20	6.54 (0.33)	4.35 (0.37)	4.49	***
$g_{\text{leaf-res}}$	1.11	6.29	2.99 (0.25)	5.67	3.63 (0.28)	1.86 (0.20)	5.48	***
$g_{\text{cuti-adaxial}}$	0.45	2.73	1.26 (0.11)	6.00	1.51 (0.14)	0.80 (0.10)	4.49	***
g_{abaxial}	0.58	3.56	1.73 (0.14)	6.14	2.12 (0.15)	1.05 (0.11)	5.79	***
$g_{\text{cuti-abaxial}}$	0.40	2.36	1.08 (0.09)	5.90	1.28 (0.11)	0.72 (0.10)	4.18	***
g_{stomata}	0.08	1.52	0.65 (0.07)	19.9	0.84 (0.08)	0.33 (0.06)	4.81	***
SS	46.4	329	165 (12.9)	7.1	133 (11.5)	219 (20.9)	-3.60	**
SD	130	1708	619 (73.8)	13.1	791 (94.7)	320 (35.5)	4.51	***
fgc	6.28	24.0	12.9 (0.93)	3.82	14.5 (1.26)	10.1 (0.78)	2.40	*
g_{wmax}	1.65	10.9	4.11 (0.38)	6.61	7.00 (0.62)	3.11 (0.27)	5.08	***
LMA	55.2	198	108 (5.90)	3.58	111 (7.01)	104 (10.9)	0.73	ns
CT_{adaxial}	1.42	12.7	4.29 (0.40)	8.92	4.70 (0.58)	3.60 (0.39)	1.30	ns
CT_{abaxial}	0.75	4.91	2.04 (0.15)	6.55	2.16 (0.21)	1.85 (0.21)	0.78	ns
CT_{total}	2.29	14.9	6.34 (0.50)	6.50	6.86 (0.71)	5.45 (0.55)	1.21	ns
$T_{\text{gs-close}}$	8.59	20.5	12.8 (0.62)	2.39	10.9 (0.38)	16.0 (0.97)	-5.61	***
THF	35.5	99.5	61.0 (3.19)	2.80	51.1 (2.12)	78.1 (4.52)	-5.85	***

The table shows overall minimum (Min), maximum (Max) and mean traits values (± SE) among species and functional groups; and the ratio of the maximum: minimum value (Ratio). For differences between functional groups, mean values of the traits are given with the *t*-test statistics for differences between deciduous and evergreen species; $^{\text{ns}}$, nonsignificant, ***, $P < 0.001$, **, $P < 0.01$, *, $P < 0.05$. Trait abbreviation as in table 2.

Table 4. Pearson correlation between diffusive and morphoanatomical traits among 30 species from Brazilian Cerrado

	A	g_{s}	E	g_{leaf}	$g_{cuti\text{-}adaxial}$	$g_{abaxial}$	$g_{cuti\text{-}abaxial}$	$g_{stomata}$	SS	SD	fgc	g_{wmax}	LMA	CT$_{adaxial}$	CT$_{abaxial}$
g_{s}	0.75***														
E	0.63***	0.93***													
g_{leaf}	0.58***	0.71***	0.66***												
$g_{cuti\text{-}adaxial}$	0.59***	0.63***	0.60***	0.96***											
$g_{abaxial}$	0.55***	0.74***	0.67***	0.98***	0.89***										
$g_{cuti\text{-}abaxial}$	0.55**	0.58***	0.55**	0.95***	0.99***	0.88***									
$g_{stomata}$	0.42*	0.70***	0.62***	0.75***	0.55**	0.86***	0.51**								
SS	-0.34^{ns}	-0.55**	-0.60***	-0.39*	-0.32^{ns}	-0.42*	-0.33^{ns}	-0.41*							
SD	0.52**	0.74***	0.74***	0.50**	0.42*	0.53**	0.36^{ns}	0.58***	-0.79***						
fgc	0.45*	0.57***	0.52**	0.37*	0.32^{ns}	0.39*	0.21^{ns}	0.47**	-0.14^{ns}	0.72***					
g_{wmax}	0.67***	0.80***	0.75***	0.64***	0.59***	0.65***	0.52**	0.63***	-0.56**	0.90***	0.81***				
LMA	0.39*	0.23^{ns}	0.13^{ns}	0.15^{ns}	0.18^{ns}	0.13^{ns}	0.13^{ns}	0.10^{ns}	0.13^{ns}	0.18^{ns}	0.44*	0.30^{ns}			
CT$_{adaxial}$	0.39*	0.20^{ns}	0.13^{ns}	0.22^{ns}	0.25^{ns}	0.19^{ns}	0.21ns	0.14^{ns}	0.24^{ns}	0.02^{ns}	0.32^{ns}	0.19^{ns}	0.70***		
CT$_{abaxial}$	0.15^{ns}	0.06^{ns}	0.02^{ns}	0.02^{ns}	0.06^{ns}	-0.01ns	0.05^{ns}	-0.06^{ns}	0.39*	-0.23^{ns}	0.06^{ns}	-0.06^{ns}	0.46**	0.75***	
CT$_{total}$	0.34^{ns}	0.18^{ns}	0.12^{ns}	0.17^{ns}	0.21^{ns}	0.14ns	0.11^{ns}	0.09^{ns}	0.30^{ns}	-0.05^{ns}	0.26^{ns}	0.13^{ns}	0.67***	0.98***	0.86***

The table shows the correlation coefficients and their significance; ^{ns}, nonsignificant, ***, $P < 0.001$, **, $P < 0.01$, *, $P < 0.05$. Trait abbreviation as in table 2.

Figure legends

Figure 1. Minimum conductance ($g_{\text{leaf-res}}$) components from a hypostomatous leaf. $g_{\text{leaf-res}}$ rates are determined by a series of parallel, and thus additive, conductances involving water leaks from the cuticle membrane of the abaxial and adaxial leaf side ($g_{\text{cuti-adaxial}}$ and $g_{\text{cuti-abaxial}}$, respectively) and stomata cells (g_{stomata}). g_{stomata}, by its turn, is composed of water leaks arising from the cuticle that covers guard cells ($g_{\text{peristomatal}}$), and from pores of incompletely closed stomata ($g_{\text{stomata-pore}}$).

Figure 2. Relationships between (a) leaf minimum conductance ($g_{\text{leaf-res}}$) and cuticular conductance from the adaxial leaf side ($g_{\text{cuti-adaxial}}$), (b) $g_{\text{leaf-res}}$ and conductance of the abaxial leaf side (g_{adaxial}), (c) g_{abaxial} and cuticle conductance of the abaxial leaf side ($g_{\text{cuti-abaxial}}$), (d) g_{abaxial} and water leaks from stomata cells (g_{stomata}), (e) relative and absolute (f) contribution of cuticle and stomata components to the overall $g_{\text{leaf-res}}$ variation across species (e) and functional groups (f) for 30 species from the Brazilian Cerrado. Significance of Person correlation coefficients: ***, $P \leq 0.001$. In e and f, different letters denote statistically significant differences between $g_{\text{leaf-res}}$ components across species (e, main plot) and within functional groups (f) through Tukey test ($P \leq 0.05$). The graph also shows the differences in $g_{\text{leaf-res}}$ components between leaf sides (e, minor plot) and functional groups (f) as denoted by *t*-test. Significance of *t*-test *P* values: ***, $P < 0.001$. Each circle represents mean values ($\log_{10}$ transformed) for each species ($n = 4$). Green and orange circles and boxes represent evergreen and deciduous species, respectively. Bars indicate means ± standard errors, and boxes indicate median, quartiles, minimum and maximum values for the relative (e) and absolute (f) conductance for each $g_{\text{leaf-res}}$ component.

Figure 3. Relationships between the leaf minimum conductance ($g_{\text{leaf-res}}$) and (a) the thickness of the cuticle from the adaxial (CT_{adaxial}), (b) abaxial (CT_{abaxial}), and (c) both leaf sides (CT_{total}) for 30 species from the Brazilian Cerrado. Significance of Pearson correlation coefficients: $^{\text{ns}}$, nonsignificant. The graph also shows (d) the differences in cuticle thinness both within and between functional groups from each leaf side, as denoted by *t*-test. Significance of t-test *P* values: ***, $P < 0.001$. Each circle represents mean values ($\log_{10}$ transformed) for each species ($n = 4$). Green and orange circles and boxes represent evergreen and deciduous species, respectively.

Boxes indicate median, quartiles, minimum and maximum values for the cuticle thickness in each leaf side.

Figure 4. Relationships between (a) the light-saturated CO_2 assimilation rate (A) and the (b) leaf minimum conductance ($g_{\text{leaf-res}}$) with stomatal conductance (g_s) for 30 species from the Brazilian Cerrado. Significance of Pearson correlation coefficients: ***, $P < 0.001$. The graph also shows the differences in $g_{\text{leaf-res}}$, A and g_s rates between functional groups (boxplots), as denoted by *t*-test. Significance of *t-test* P values: ***, $P < 0.001$. Each circle represents mean values ($\log_{10}$ transformed) for each species ($n = 4$). Green and orange circles and boxes represent evergreen and deciduous species, respectively.

Figure 5. Relationships between stomatal conductance (g_s) with (a) stomatal size (SS), (b) stomatal density (SD), (c) fraction of epidermis allocated to stomata (f_{gc}), and (d) theoretical maximum stomatal conductance (g_{wmax}), and between leaf minimum conductance ($g_{\text{leaf-res}}$) with SS (e), (f) SD, (g) f_{gc}, and (h) g_{wmax} for 30 species from the Brazilian Cerrado. Significance of Pearson correlation coefficients: $^{\text{ns}}$, nonsignificant, ***, $P < 0.001$, **, $P < 0.01$, *, $P < 0.05$. The graph also shows the differences in diffusive and stomatal morphoanatomical traits between functional groups, as denoted by *t*-test. Significance of t-test P values: ***, $P < 0.001$. Each circle represents mean values ($\log_{10}$ transformed) for each species ($n = 4$). Green and orange circles represent evergreen and deciduous species, respectively.

Figure 6. Principal component analysis (PCA) with the mean values of physiological and morphoanatomical leaf traits of 30 species from Brazilian Cerrado. Figures show the variation in trait scores (a) and species scores (b) along the first two PCA axes with the percentages of explained variation given. Green and orange circles represent evergreen and deciduous species, respectively. Variables were log10-transformed before analysis. For full species names, see Table 1. Trait abbreviation as in Table 2.

Figure 7. Conceptual model showing the trade-offs underlying the variability in leaf minimum conductance across species from the Brazilian Cerrado. Evergreen species tend to present a more conservative growth strategy, which involves the construction of leaves with fewer and larger stomata (lower SS and higher SD, respectively), resulting in a lower CO_2 diffusion (g_s). Although

this strategy leads to a lower CO_2 assimilation capacity (A), it also prevents the excessive water leaks ($g_{\text{leaf-res}}$). On the other hand, the fast-growing strategy of deciduous species involves the investment in numerous small stomata (higher *SD* and lower *SS*), which result in higher CO_2 diffusion capacity. However, although this strategy maximizes the CO_2 assimilation rate, it also leads to higher water loss thought stomata leaks.

Figure 8. Relationships between (a) modelled time to stomatal closure ($T_{\text{gs-close}}$) with stomatal conductance (g_s), and (b) modelled time to hydraulic failure (THF) with minimum leaf conductance ($g_{\text{leaf-res}}$) for 30 species from the Brazilian Cerrado. The graph also shows the variation in mean $T_{\text{gs-close}}$ and THF values between functional groups (c), as denoted by *t*-test. Significance of *P* values for *t*-test and Pearson correlation coefficients: ***, $P < 0.001$. Each circle represents mean values ($\log_{10}$ transformed) for each species ($n = 4$). Green and orange circles and bars represent evergreen and deciduous species, respectively.

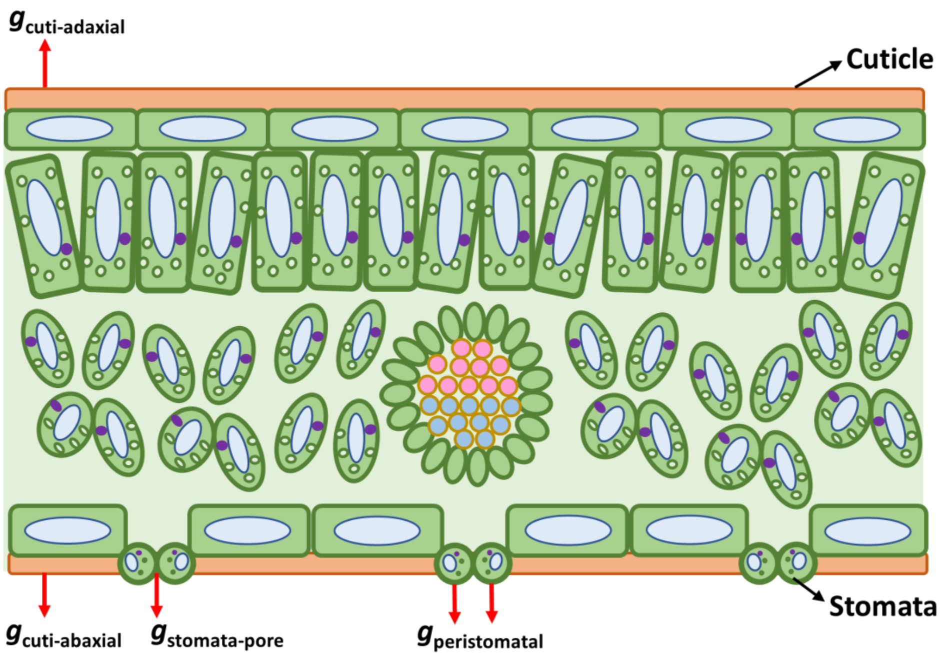

nph_16941_f1.tif

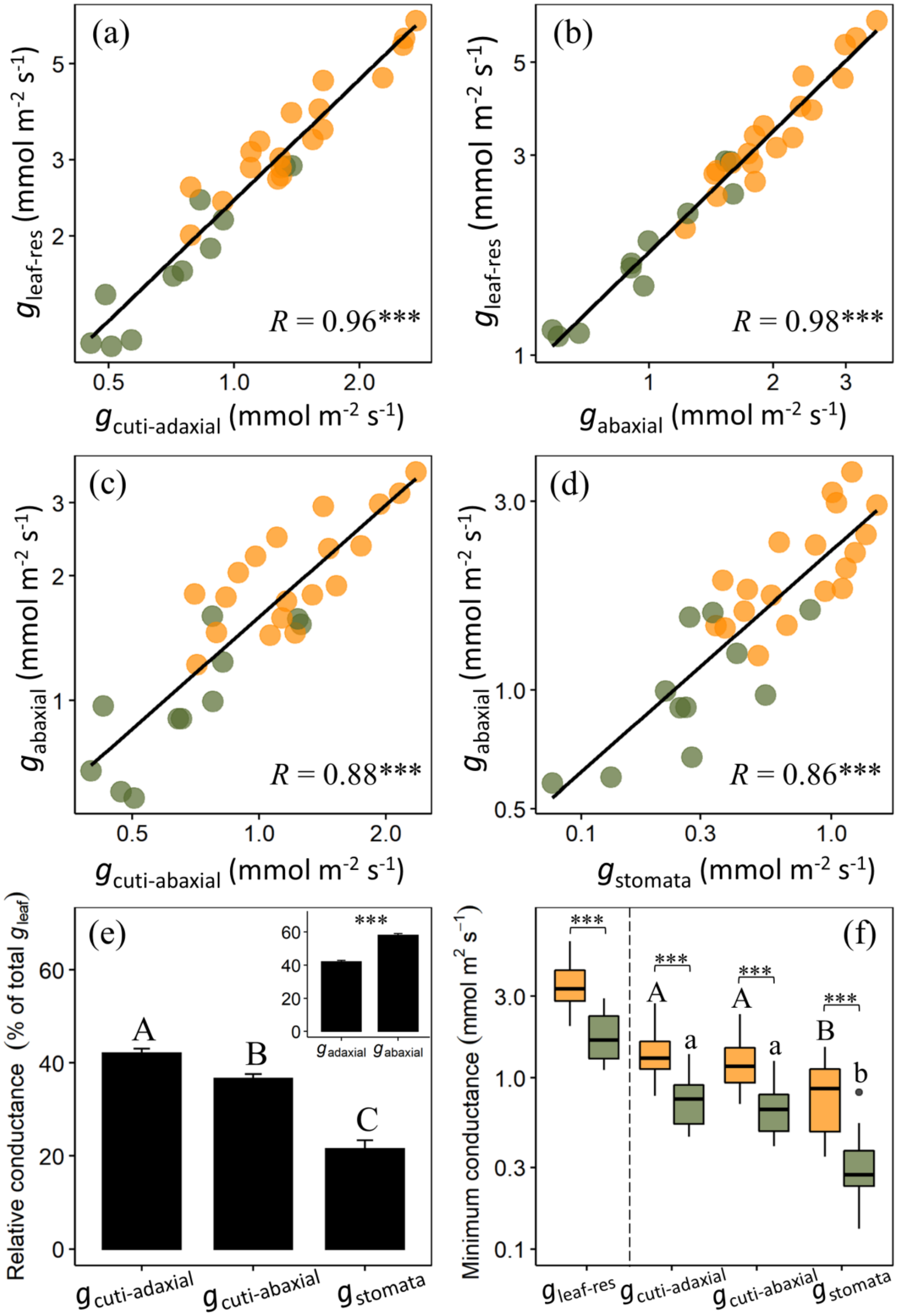

nph_16941_f2.tif

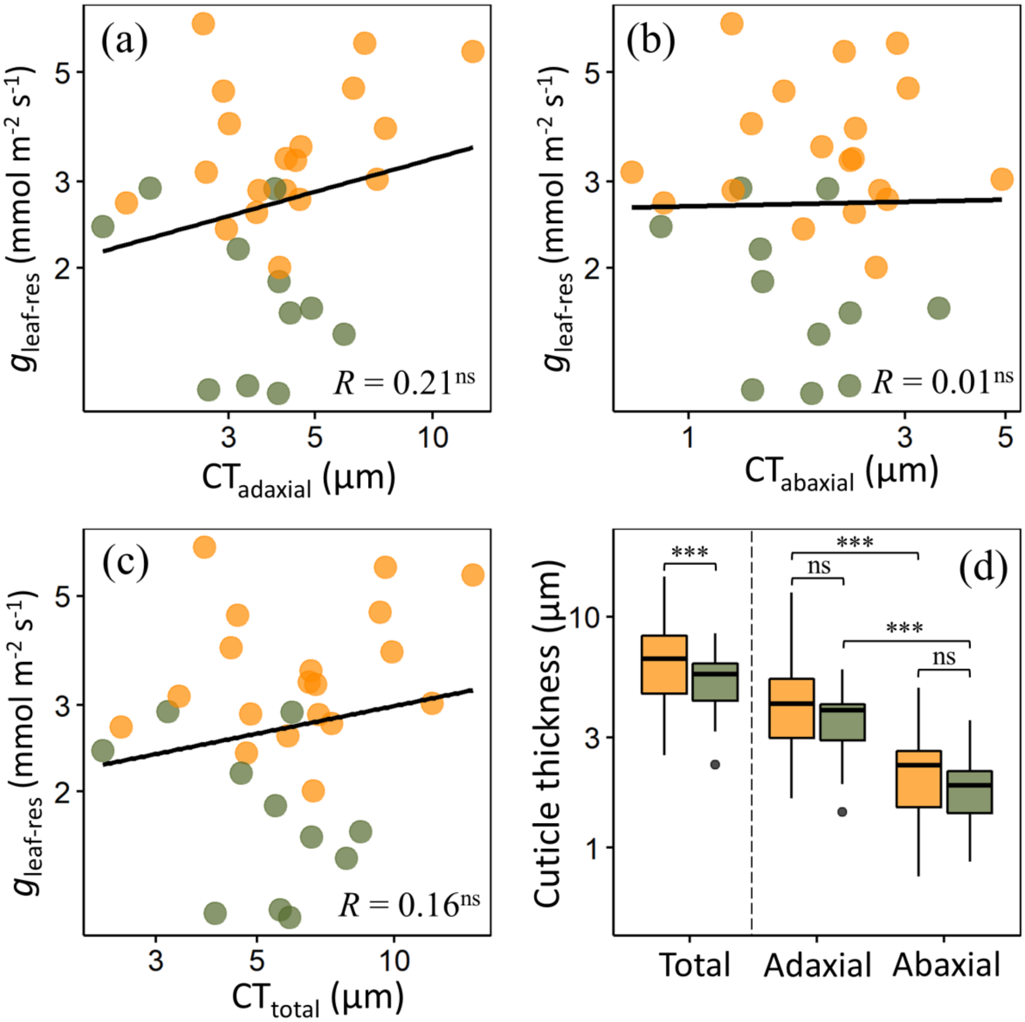

nph_16941_f3.tif

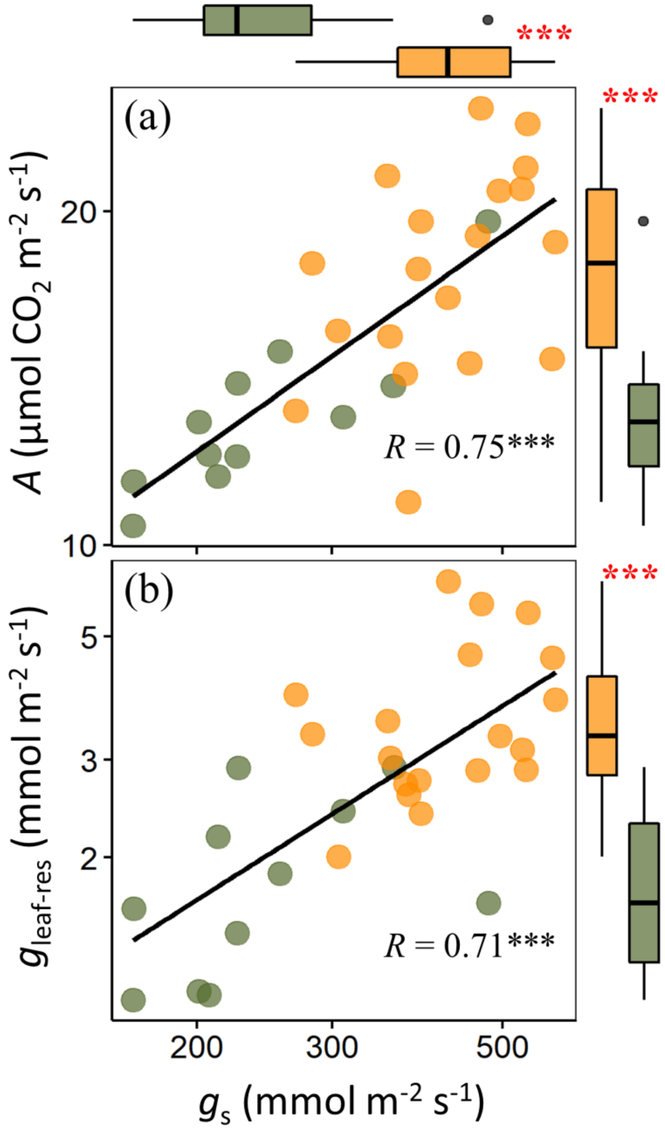

nph_16941_f4.tif

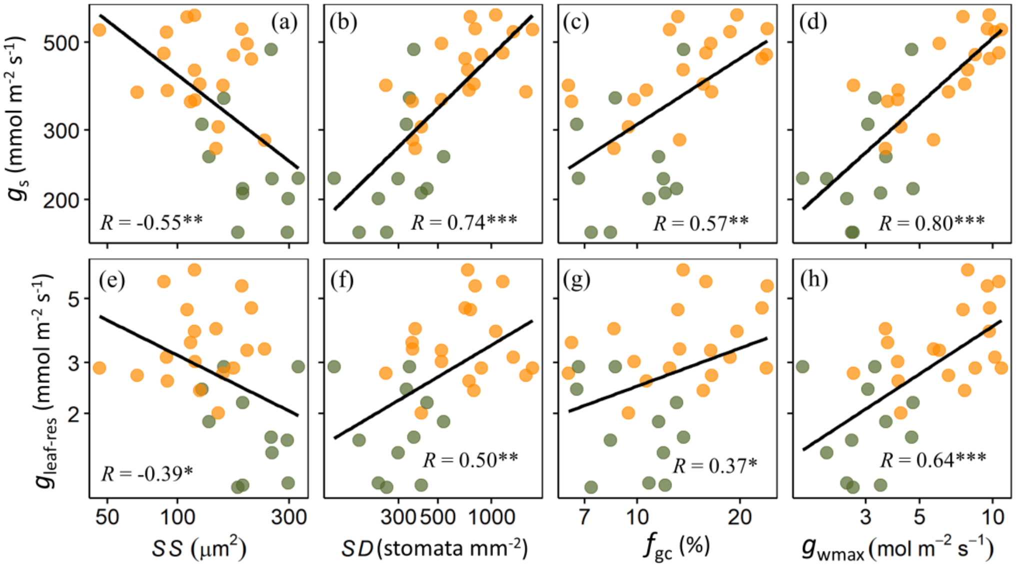

nph_16941_f5.tif

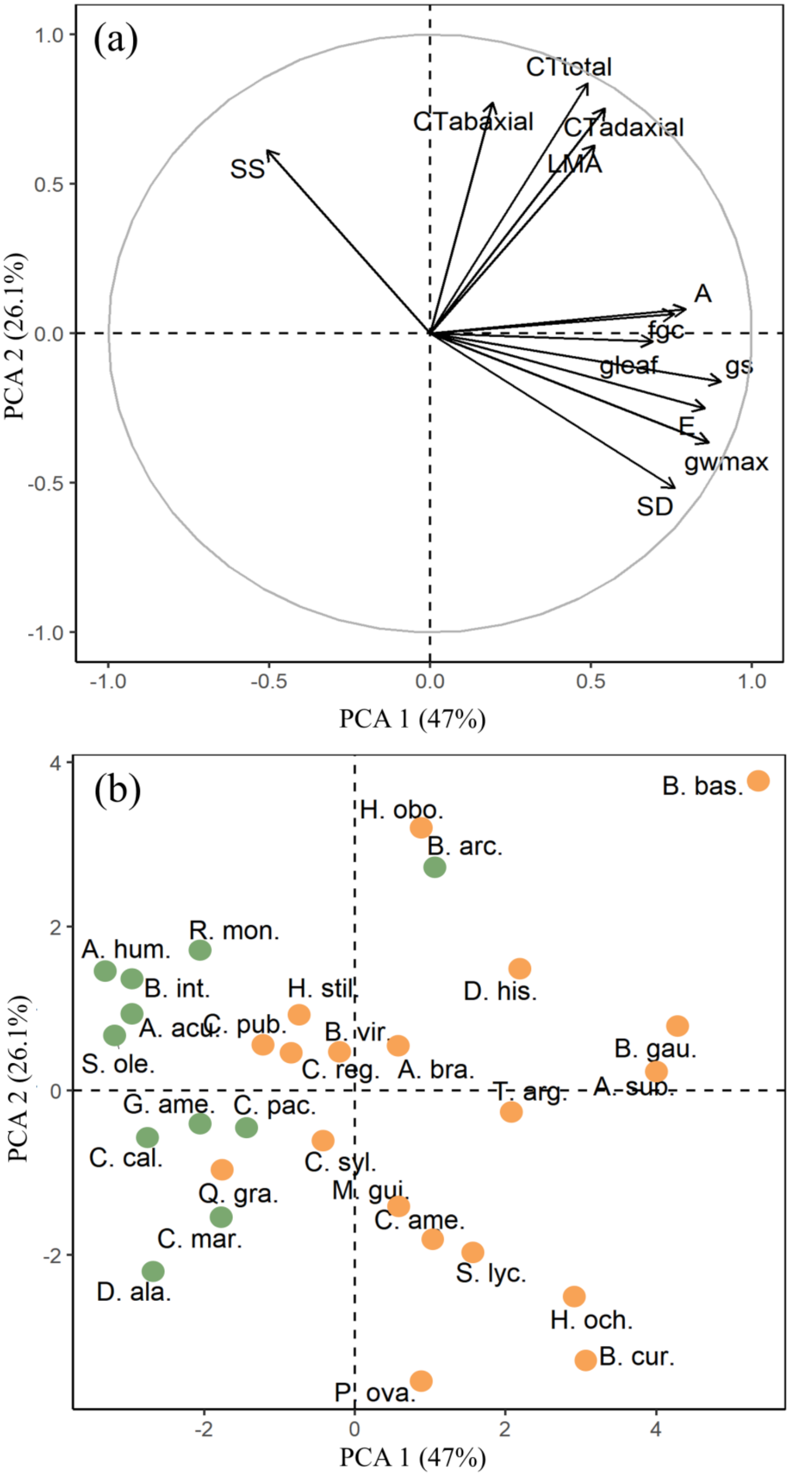

nph_16941_f6.tif

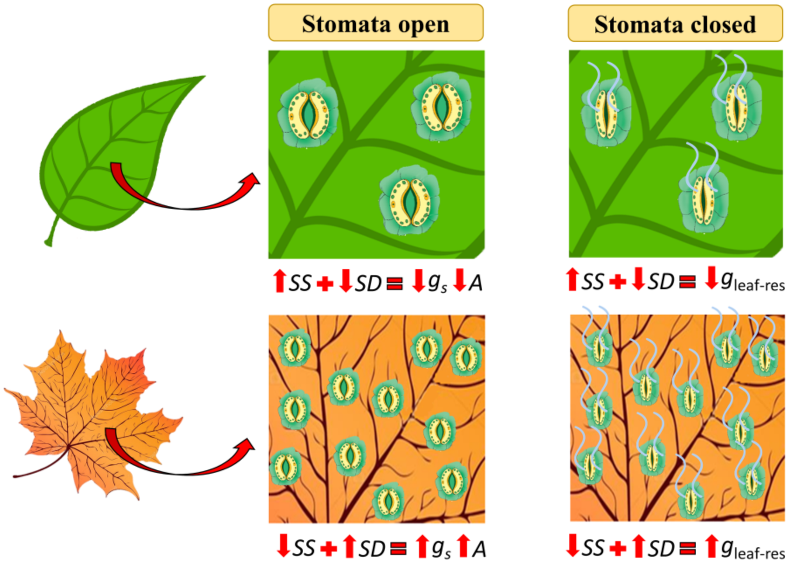

nph_16941_f7.tif

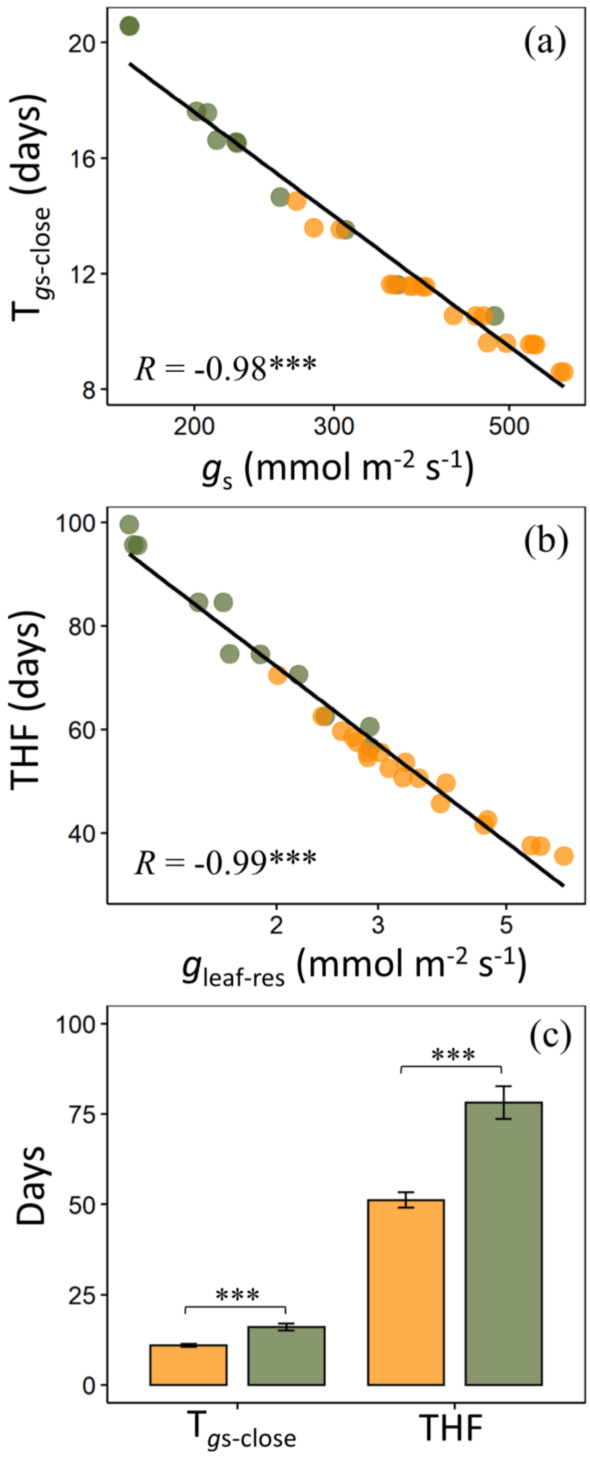

nph_16941_f8.tif